# Proton form factor from 0.15 to 0.79 fm$^{-2}$ *

J. J. Murphy, II, Y. M. Shin, and D. M. Skopik
*Saskatchewan Accelerator Laboratory, University of Saskatchewan, Saskatoon, Canada S7N OWO*

(Received 7 January 1974)

The absolute electron-proton elastic scattering cross section has been measured by detecting the recoil protons. The proton charge form factor has been extracted for values of the square of the momentum transfer between 0.15 and 0.79 fm$^{-2}$. The rms charge radius determined from these measurements is 0.81 ± 0.04 fm.

[NUCLEAR REACTIONS $^1$H($e, p$), $E$ = 55–130 MeV, measured $\sigma(E; E_p, \theta)$; deduced charge form factor, rms charge radius.]

## I. INTRODUCTION

Accurate measurement of the absolute electron-proton elastic scattering cross section is fundamental in the investigation of nuclear structure. Form factors derived from this cross section represent information about the spatial distribution of charge and current within the proton. Furthermore, in many electron scattering experiments on nuclei more complex than hydrogen the cross sections obtained are normalized to the hydrogen cross section.

The proton form factors are usually measured by electron scattering experiments in which electrons, after scattering from the hydrogen nucleus, are detected. Figure 1 shows the results of such experiments[1-4] for values of the momentum transfer $q^2$ less than 1 fm$^{-2}$. In this paper we describe work carried out at the University of Saskatchewan linear accelerator laboratory in which the recoil protons rather than the scattered electrons were detected. The advantages of this alternative approach are several. The nonrelativistic protons are appreciably easier to collimate than the relativistic electrons. The signal-to-background ratio of the experiment is better because there are many fewer stray protons than electrons in the experimental area. The radiative correction that must be made to the data is smaller for the detection of protons than for the detection of electrons. Finally, since any systematic errors of the two approaches are expected to be different, each experiment complements and checks the other.

We have made absolute measurements of the proton's electric form factor at 11 values of $q^2$ from 0.15 to 0.79 fm$^{-2}$. From our values for the form factor we deduce an rms charge radius for the proton of 0.81 ± 0.04 fm, which is in agreement with the generally accepted value of 0.805 ± 0.011 fm,[5] which was determined using data for $q^2 \leq 3$ fm$^{-2}$ from a number of experiments. Our value, however, disagrees with the larger value recently reported by a group at Mainz.[6] This group reports a charge radius of 0.88 ± 0.03 fm when their data are analyzed with a two-double-pole model, and 0.92 ± 0.02 fm when analyzed with a four-single-pole model.

## II. EXPERIMENTAL ARRANGEMENT

The experimental arrangement has been described previously.[7] Since no important changes were made in the experimental apparatus or procedures for this experiment, only a brief description is given here.

The energy-analyzed electron beam (±1% energy spread) from the University of Saskatchewan linear accelerator was incident on a gaseous hydrogen target. The target consisted of a right circular cylinder 2.54 cm in radius and 3.50 cm high, oriented with its axis of rotation perpendicular both to the electron beam and to the path of the detected recoil protons. The walls of the target were 6.4 μm Havar.[8] The target was filled with 2.00 ± 0.02 atm of hydrogen measured with a tem-

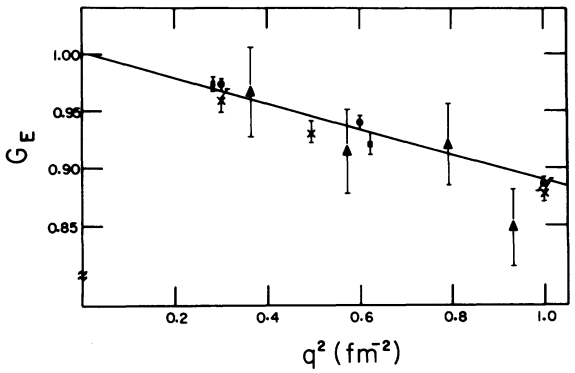


FIG. 1. Low $q$ measurements of the proton charge form factor: ●, Ref. 1; ■, Ref. 2; ▲, Ref. 3; X, Ref. 4. The solid line corresponds to $\langle r^2 \rangle^{1/2} = 0.81$ fm.

TABLE I. Sources of scale error.

| Item | Uncertainty (%) |
|---|---|
| Spectrometer solid angle | ±2 |
| Momentum acceptance | ±2 |
| Number of target nuclei | ±3 |
| Incident electron flux | ±2 |
| Total | 4.6 |

perature-compensated Bourdon tube gauge and permanently sealed.

The recoil protons were detected by a spectrometer which consists of five surface barrier silicon detectors mounted in the focal plane of a 127° double-focusing magnet. The energy calibration, solid angle, and lateral efficiency of the spectrometer were determined by the use of 5.49-MeV $\alpha$ particles from an $^{241}$Am source. The procedures are described in detail in Ref. 7. The uncertainties associated with these measurements are tabulated in Table I.

Signals from the five focal plane detectors, after amplification, were fed into five analog-to-digital converters (ADC) associated with an XDS 920 computer. The ADC's were gated on for 4 $\mu$sec by the linac master trigger for each beam burst. A typical pulse height spectrum for a single detector is shown in Fig. 2. Note that only the peak corresponding to protons is present. This was taken as evidence of the purity of the target gas.

Beam current was measured by a nonintercepting SLAC-type ferrite monitor[9] whose response was checked periodically with a Faraday cup. Deviations in the ferrite's response and linearity never exceeded 2%.

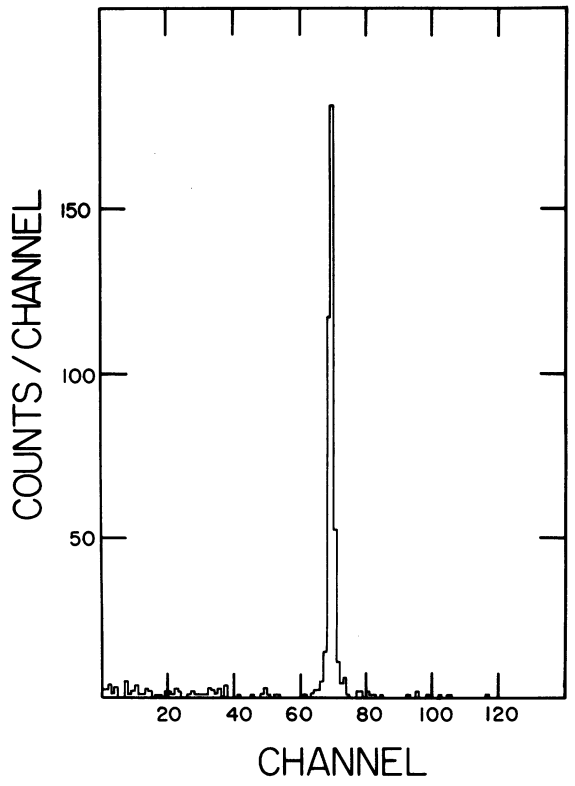


FIG. 2. Pulse-height spectrum for detector 3 corresponding to a proton energy of 5.6 MeV. Note the absence of all peaks except that corresponding to protons.

## III. DATA ANALYSIS

Since the procedures and formulas used in reducing the experimental data to values for the form factor are less widely known for the case of proton detection than for that of electron detection, an effort is made in this section to state the relevant formulas carefully.

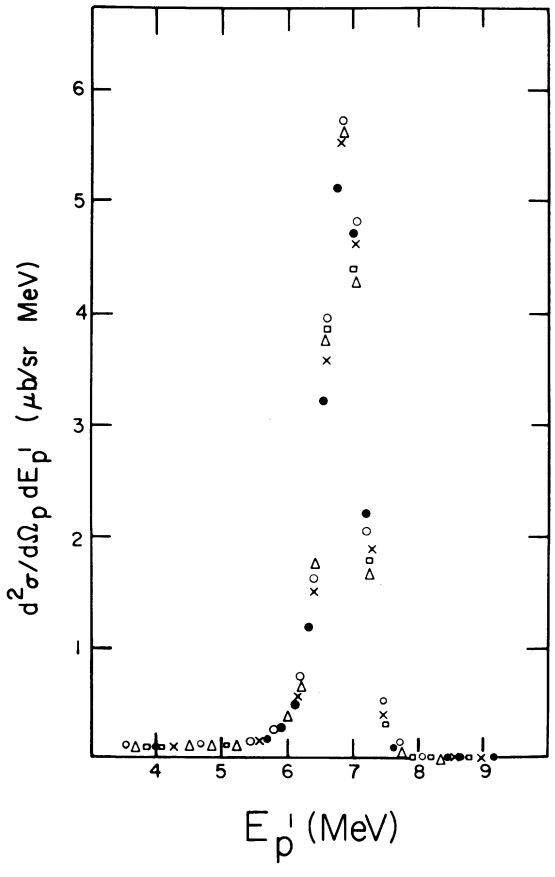


FIG. 3. The doubly differential cross section $d^2\sigma/d\Omega_p dE_p'$ as a function of $E_p'$. The data shown are for $E_0 = 89.7$ MeV and $\theta_p = 45°$ corresponding to a momentum transfer squared of 0.347 fm$^{-2}$. The five symbols correspond to the five focal plane detectors.

For a given spectrometer angle and detected proton energy $\theta_p$ and $E_p'$, the experimental cross section is

$$\frac{d^2\sigma}{d\Omega_p\, dE_p'} = \frac{C_p(\theta_p, E_p')}{\Delta E_p' \Delta\Omega_p\, n_t(\theta_p)}$$

where $C_p(\theta_p, E_p')$ is the number of protons detected per incident electron, $\Delta\Omega_p$ is the spectrometer solid angle and $n_t(\theta_p)$ is the number of target nuclei/cm$^2$; $n_t(\theta_p)$ is proportional to the measured spectrometer lateral efficiency and $\csc(\theta_p)$. The energy acceptance of the spectrometer is given by $\Delta E_p'$. Figure 3 shows $d^2\sigma/d\Omega_p\, dE_p'$ as a function of $E_p'$, the kinetic energy of the detected proton. The data shown are for $\theta_p = 45°$ and incident electron energy of 89.7 MeV, corresponding to a momentum transfer squared of 0.347 fm$^{-2}$, but are typical of all the data taken.

In order to obtain the proton form factor from the measured cross section we require $d\sigma/d\Omega_p$. These two cross sections are related by

$$\frac{d\sigma}{d\Omega_p} = R(E_{\min}) \int_{E_{\min}}^{\infty} (d^2\sigma/d\Omega_p\, dE_p') dE_p' \qquad (1)$$

where $R(E_{\min})$ is the radiative correction. The radiative correction takes into account both the experimental fact that there is a low-energy cutoff ($E_{\min}$) to the integration and the fact that the experimental cross section includes contributions from the diagrams of Figs. 4(a) and 4(b) whereas the theoretical cross section, which includes the form factors, is computed for only the diagram of Fig. 4(a). The radiative correction when protons are detected has been calculated by Meister and Yennie.[10] They find

$$R(E_{\min}) = 1 - \delta\,,$$

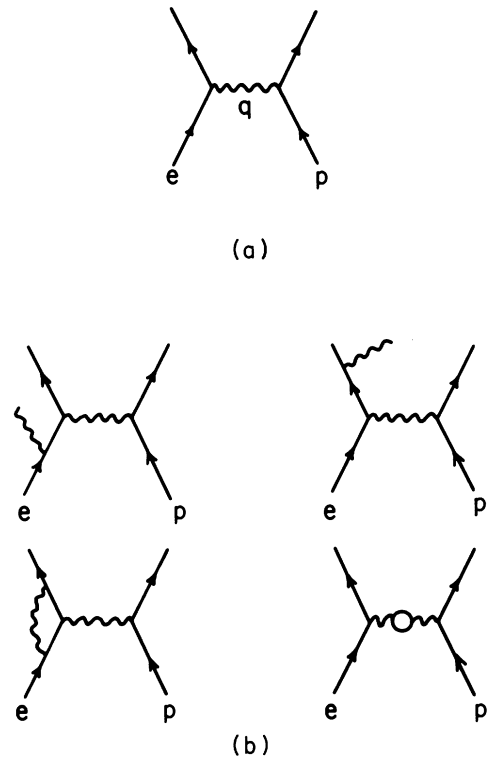


FIG. 4. Feynman diagrams for elastic electron scattering. The experimental measurement includes contributions from (b) as well as (a), whereas the Rosenbluth formula includes only the contribution from (a).

where

$$\delta \cong \frac{\alpha}{\pi}\left\{\left[\ln\left(\frac{2\vec{p}_1\cdot\vec{p}_3}{m^2}\right)-1\right]\ln\Lambda + \frac{17}{12}\ln\left(\frac{2\vec{p}_1\cdot\vec{p}_3}{m^2}\right) - \frac{28}{9} - \frac{1}{2}\ln^2\Lambda - \frac{3}{4}\ln\Lambda + \ln\eta\ln\left[\frac{(\vec{p}_1\cdot\vec{p}_3)^2}{M^2E_1E_3}\Lambda^4\right]\right.$$
$$\left. - [\ln(2E_1/M)]^2 + [\ln(2E_3/M)]^2 + \left[\frac{E_4}{p_4}\ln\left(\frac{E_4+p_4}{M}\right)-1\right]\ln\left[\frac{(\vec{p}_1\cdot\vec{p}_3)^2}{M^2E_1E_3}\Lambda^2\right] + \frac{3}{2}\ln\left(\frac{2E_4}{M}\right) - \frac{1}{2}\ln^2\eta\right\},$$

$$\Lambda = [(E_1+M)/E_4](\Delta p_4/p_4)\,, \quad \eta = E_1/E_3\,.$$

The subscripts 1, 3, and 4 refer to the incident electron, scattered electron, and recoil proton, respectively. The difference in four-momentum between the elastic peak and the integration cutoff energy is $\Delta p_4$. All kinematic quantities were calculated using the spectrometer angle $\theta_p$ and the proton energy at the peak of $d^2\sigma/d\Omega_p\, dE_p'$. This proton energy was obtained from the detected proton energy at the peak by using the Bethe-Bloch formula to compute the energy loss of the proton in escaping from the gas target. The initial electron energies calculated in this way agreed with the linac calibration energies to better than 2% in all cases.

Before carrying out the integration and applying the radiative correction as indicated in Eq. (1), we subtracted from $d^2\sigma/d\Omega_p\, dE_p'$ a small background linear in $E_p'$. This background was obtained by fitting to the cross section above and below the elastic peak and was consistent with the proton spectra measured with an empty target. The operations indicated in Eq. (1) were carried out for a wide range

of integration cutoff energies from below the elastic peak to the experimental cutoff energy. The values obtained for $d\sigma/d\Omega_p$ were independent of $E_{\min}$ to within less than ±1%.

The Rosenbluth formula[11] for the electron scattering cross section when the scattered electrons are detected is

$$\frac{d\sigma}{d\Omega_e} = \sigma_{NS}\left[(G_E^2 + \tau G_M^2)/(1+\tau) + 2\tau G_M^2 \tan^2\tfrac{1}{2}\theta_e\right],$$

where

$$\sigma_{NS} = \frac{\alpha^2}{4E_0^2 \sin^4\tfrac{1}{2}\theta_e} \cos^2\tfrac{1}{2}\theta_e \frac{1}{1+(2E_0/M)\sin^2\tfrac{1}{2}\theta_e},$$

$$\tau = q_\mu^2/4M^2,$$

and $G_E$ and $G_M$ are the electric and magnetic form factors, $q_\mu^2$ is the four-momentum transfer squared, $M$ is the proton mass, $\theta_e$ is the electron scattering angle, $E_0$ is the incident electron energy, and $\alpha$ is the fine structure constant. The units are such that $\hbar = c = 1$. The formula neglects terms of order $m/M$ and $T/M$ where $m$ is the electron mass and $T$ is the proton kinetic energy.

In order to extract a form factor from our measured cross section we require the corresponding formula for the case in which the recoil proton is detected. If in deriving the Rosenbluth formula one integrates over the scattered electron variables rather than the recoil proton variables, the required result is obtained. Equivalently one can multiply the Rosenbluth formula by $d\Omega_e/d\Omega_p$ and express the results in terms of $\theta_p$ rather than $\theta_e$. In either case one obtains

$$\frac{d\sigma}{d\Omega_p} = \sigma_{NS}\frac{G_E^2 + \tau G_M^2}{1+\tau} + 2\tau G_M^2\left(\frac{1}{1+\rho}\right)^2 \cot^2\theta_p$$

$$= \sigma_{NS} G^2,$$

where

$$\sigma_{NS} = \left(\frac{\alpha}{E_0}\right)^2 \frac{1+\rho^4\sin^2\theta_p}{\cos^3\theta_p} \frac{1}{1+2\rho+\rho^2\sin^2\theta_p},$$

$$\rho = E_0/M.$$

In extracting $G_E$ from $d\sigma/d\Omega_p$ we assumed $G_M = 2.79G_E$. This assumption is consistent with our data and is supported by earlier results[5,12] for the values of $q^2$ in this experiment.

## IV. RESULTS AND CONCLUSIONS

Table II summarizes the results of our experiment. The errors attached to $G_E$ include both statistical counting errors and the uncertainties resulting from variations in $d\sigma/d\Omega_p$ as a function of the integration cutoff energy. The statistical counting errors were ≤0.2% for all data points. The uncertainties resulting from the variations of $d\sigma/d\Omega_p$ with integration cutoff energy were estimated from the spread in values of $d\sigma/d\Omega_p$ obtained as the cutoff energy was varied. These uncertainties were combined in quadrature with the statistical errors to obtain the errors given for $G_E$ in Table II.

TABLE II. Experimental results. The ratio $G/G_E$ is a measure of the magnetic contribution to the cross section.

| $q^2$ (fm$^{-2}$) | $E_0$ (MeV) | $\theta_p$ (deg) | $G/G_E$ | $G_E$ |
|---|---|---|---|---|
| 0.150 | 57.3 | 45 | 1.017 | 0.981 ± 0.005 |
| 0.295 | 82.2 | 45 | 1.032 | 0.969 ± 0.005 |
| 0.297 | 82.4 | 45 | 1.032 | 0.966 ± 0.003 |
| 0.347 | 89.7 | 45 | 1.037 | 0.961 ± 0.003 |
| 0.390 | 95.6 | 45 | 1.041 | 0.962 ± 0.003 |
| 0.396 | 96.4 | 45 | 1.042 | 0.955 ± 0.003 |
| 0.440 | 102.2 | 45 | 1.046 | 0.951 ± 0.003 |
| 0.493 | 108.7 | 45 | 1.051 | 0.942 ± 0.004 |
| 0.530 | 90.4 | 30 | 1.125 | 0.939 ± 0.009 |
| 0.678 | 118.6 | 40 | 1.082 | 0.922 ± 0.004 |
| 0.794 | 129.5 | 40 | 1.099 | 0.914 ± 0.004 |

Since to order $q^2$ the exponential, Yukawa, and Gaussian expressions for the charge distribution all yield $G_E(q^2) = a + bq^2$, we fitted our data to this form. The weighted least-squares fit results in[13]

$$a = \frac{1}{\Delta}\sum\frac{q_i^4}{\Delta G_i^2}\sum\frac{G_i}{\Delta G_i^2} - \sum\frac{q_i^2}{\Delta G_i^2}\sum\frac{q_i^2 G_i}{\Delta G_i^2},$$

$$b = \frac{1}{\Delta}\sum\frac{1}{\Delta G_i^2}\sum\frac{q_i^2 G_i}{\Delta G_i^2} - \sum\frac{q_i^2}{\Delta G_i^2}\sum\frac{G_i}{\Delta G_i^2},$$

$$\Delta = \sum\frac{1}{\Delta G_i^2}\sum\frac{q_i^4}{\Delta G_i^2} - \left[\sum\frac{q_i^2}{\Delta G_i^2}\right]^2,$$

$$(\Delta a)^2 = \frac{1}{\Delta}\sum\frac{q_i^4}{\Delta G_i^2},$$

$$(\Delta b)^2 = \frac{1}{\Delta}\sum\frac{1}{\Delta G_i^2}.$$

The values obtained were : $a = 1.000 \pm 0.003$, $b = 0.110 \pm 0.007$ fm$^2$, with a reduced $\chi^2$ of 0.6. The data and fitted curve are shown in Fig. 5.

The charge radius is given by

$$\langle r^2\rangle = \frac{-6}{G_E(0)}\left[\frac{d}{dq^2}G_E(q^2)\right]_{q^2=0}.$$

Using the values of the coefficients obtained in our fit, we find $\langle r^2\rangle^{1/2} = 0.81 \pm 0.04$ fm. A fit of the data was also made to the form

$$G_E(q^2) = a + bq^2 + \lambda q^4.$$

However, the addition of this $\lambda$ term did not improve the fit. Moreover, from the fitted value $0.007 \pm 0.032$ fm$^4$ one cannot distinguish among the exponential, Yukawa, and Gaussian forms of the

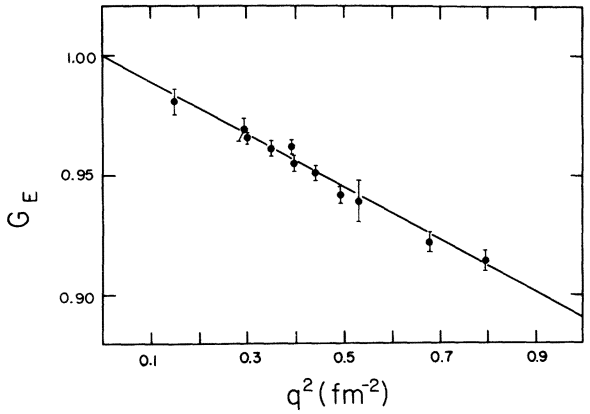


FIG. 5. Proton charge form factor as a function of $q^2$. The solid line is a least-squares fit to the data points. The corresponding rms charge radius of the proton is $0.81 \pm 0.04$ fm.

charge distribution. This is not surprising because at the low-momentum transfers of this experiment one does not expect $G_E$ to be model-dependent.

Our result $\langle r^2 \rangle^{1/2} = 0.81 \pm 0.04$ fm is in excellent agreement with previous results from electron scattering experiments.[5] This agreement between our experiment in which the recoil protons were detected and those in which the scattered electrons were detected is particularly satisfying. We can offer no explanation for the disagreement between our result and the recent result of the group at Mainz.[6]

We wish to thank Dr. E. L. Tomusiak for many valuable discussions concerning the results, and the accelerator staff for their assistance during the experiment.

---

*Work supported by the Atomic Energy Control Board of Canada.

[1]D. J. Drickey and L. N. Hand, Phys. Rev. Lett. 9, 521 (1962).

[2]D. Yount and J. Pine, Phys. Rev. 128, 1842 (1962).

[3]F. Bumiller, M. Croissiaux, E. Dally, and R. Hofstadter, Phys. Rev. 124, 1623 (1961).

[4]B. Dudelzak, G. Sauvage, and P. Lehmann, Nuovo Cimento 28, 18 (1963).

[5]L. N. Hand, D. G. Miller, and R. Wilson, Rev. Mod. Phys. 35, 335 (1963).

[6]F. Borkowski, P. Penser, G. Simon, V. H. Walther, and R. D. Wendling, in *International Conference on Photonuclear Reactions and Applications, Asilomar, California, 1973*, edited by B. L. Berman (Lawrence Livermore Laboratory, University of California, Livermore, California, 1973), p. 881; H. Averding, Results of electron-scattering experiments at Mainz University 300-MeV Electron Linear Accelerator, 1974 (unpublished).

[7]D. M. Skopik, Y. M. Shin, M. C. Phenneger, and J. J. Murphy, II, Phys. Rev. C 9, 531 (1974).

[8]Trademark, Precision Metals Division, Hamilton Watch Company, Lancaster, Pennsylvania.

[9]D. Olsen, Stanford Linear Accelerator Center Technical Note No. SLAC-TN-65-66 (unpublished).

[10]N. Meister and D. R. Yennie, Phys. Rev. 130, 1210 (1963).

[11]M. N. Rosenbluth, Phys. Rev. 79, 615 (1950).

[12]H. Theissen and W. Schutz, Z. Phys. 266, 33 (1974).

[13]Philip R. Bevington, *Data Reduction and Error Analysis for the Physical Sciences* (McGraw-Hill, Toronto, 1969), Chap. 6.